Towards a Time-Dependent Probabilistic Seismic Hazard Assessment: the case of Calabria, Italy

Aybige AKINCI, Paola VANNOLI, Giuseppe FALCONE, Matteo TARONI, Mara Monica TIBERTI, Maura MURRU, Pierfrancesco BURRATO, and Maria Teresa MARIUCCI

Istituto Nazionale di Geofisica e Vulcanologia, Via di Vigna Murata 605, 00143 Rome, Italy, Tel.: +39 06 51860403, aybige.akinci@ingv.it

ABSTRACT

In this study, we improve the knowledge on the seismotectonic framework of the Calabrian region by using any available geologic, tectonic, paleoseismic, and macroseismic information in the literature. We construct a PSHA model based on the long-term recurrence behavior of seismogenic faults together with the spatial distribution of earthquakes observed in historic time (Akinci et al., 2009; Akinci, 2010). We derive the characteristic earthquake model for those sources that could rupture the entire fault segment (full-rupture) independently with a single maximum magnitude. However, the floating rupture model is applied to those earthquakes whose location is not known with sufficient precision and correlated to longer fault systems, assuming that any of those earthquakes can rupture anywhere inside that zone (floating partial-rupture) with uniform probability.

In order to express the time dependence of the seismic processes to predict the future ground motions in the region, we use a Brownian Passage Time (BPT) model characterized by a mean recurrence, aperiodicity, or uncertainty in the recurrence distribution and elapsed time since the last earthquake (Akinci et al., 2010). Besides, we consider a physical parameter of the static Coulomb stress change (ΔCFF) due to the fault interaction from earthquakes that influence the probability of earthquake occurrence and adopt a model built on the fusion of BPT model (BPT+ΔCFF).
We present our results for both time-dependent and Poisson models in terms of maps of Peak Ground Acceleration (PGA) for 10% probability of exceedance in 50 yrs in Calabria through a logic tree approach.

The hazard may increase by more than 20% or decrease by as much as 50% depending on the different occurrence model. Seismic hazard in terms of PGA decreases about 20% in the Messina Strait, where a recent major earthquake took place, with respect to traditional time-independent estimates. PGA near the city of Cosenza reaches ~0.36 g for the time-independent model and 0.40g for the case of the time-dependent one (i.e. a 15 % increase). Both the time-dependent and time-independent models for the period of 2015-2065 demonstrate that the city of Cosenza and surrounding areas bear the highest seismic hazard in Calabria.

SEISMIC CATALOGS

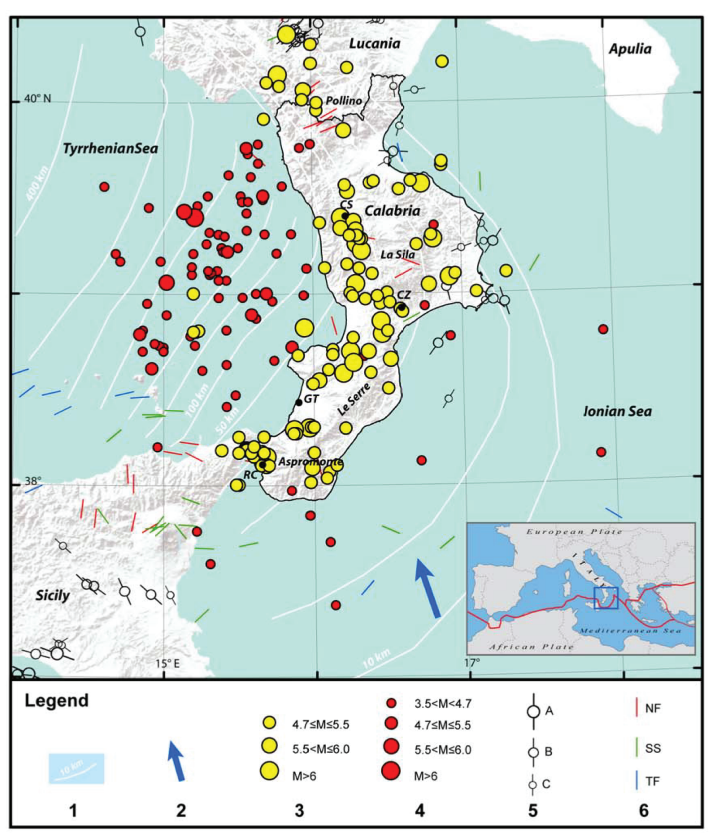

SEISMOGENIC SOURCES

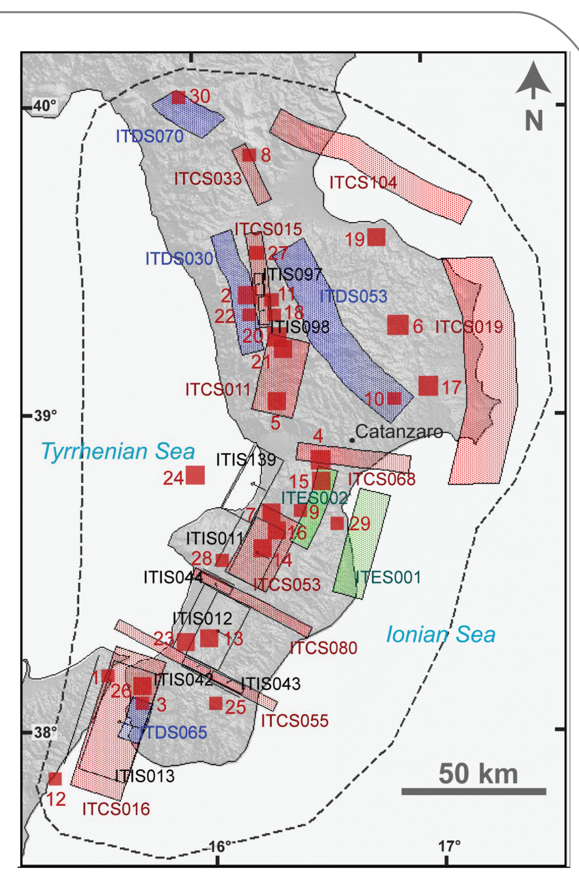

Seismotectonic framework of the study area. Legend: 1- isobaths of the subduction; 2-plate motion from Nuvel 1A; 3- historical earthquakes from CPTI 11 catalog (Rovida et al., 2011); 4- instrumental seismicity with depth h >30 km from CSI 1.1 (Castello et al., 2006), M is the moment magnitude; 5- minimum horizontal stress orientations from borehole breakouts, quality ranked, and from 6- earthquake focal mechanisms (NF= normal fault, SS= strike-slip, TF= thrust The seismogenic source model used in this study: Individual Sources (IS) in black; Composite Sources (CS) in purple; Debated Sources (DS) in blue; Exploratory Source (ES) in green. The IS and CS sources are from the Database DISS (DISS Working Group, 2015); the DS were parameterized and the ES were developed in this study. The historical earthquakes are shown as red squares and listed in Table 1.fault regime) after Montone et al., 2012. CS: Cosenza; CZ: Catanzaro; GT: Gioia Tauro; RC: Reggio Calabria.

ID	Year	Mo	Da	Ho	Mi	Se	Ax	$M_w$def	Sources	Rank
1	1172	9	26	13	40		Messina	5.57	ITCS016	C
2	1184	5	24				Valle del Crati	6.74	ITDS053	E
3	1509	2	25	22	20		Calabria meridionale	5.57	ITDS065	E
4	1626	4	4	12	45		Girifalco	6.03	ITCS068	C
5	1638	3	27	15	5		Calabria	7.03	ITCS111	B
6	1638	6	8	9	45		Crotonese	6.89	ITDS053	D
7	1659	11	5	22	15		Calabria centrale	6.55	ITES001	F
8	1693	1	8	22	15		Calabria settentrionale	5.67	ITCS033	C
9	1743	12	7	0	5		Calabria centrale	5.68	ITES002	F
10	1744	3	21	20			Crotonese	5.74	ITDS053	D
11	1767	7	14	1	5		Cosentino	5.98	ITIS097, ITCS015	A
12	1780	3	28	22	15		Taormina	5.55	ITCS016	C
13	1783	2	5	12			Calabria	7.02	ITIS012	A
14	1783	2	7	13	10		Calabria	6.62	ITIS011, ITCS053	A
15	1783	3	28	18	55		Calabria	6.98	ITES002	F
16	1791	10	13	1	20		Calabria centrale	6.03	ITCS053	B
17	1832	3	8	18	30		Crotonese	6.59	ITCS019	C
18	1835	10	12	22	35		Cosentino	5.83	ITIS098, ITCS015	A
19	1836	4	25	0	20		Calabria settentrionale	6.2	ITCS104	E
20	1854	2	12	17	50		Cosentino	6.21	ITDS030	E
21	1870	10	4	16	55		Cosentino	6.1	ITCS111	C
22	1886	3	6				Cosentino	5.55	ITCS015	C
23	1894	11	16	17	52		Calabria meridionale	6.07	ITIS042, ITCS055	A
24	1905	9	8	1	43		Calabria meridionale	7.04	ITIS139	A
25	1907	10	23	20	28		Calabria meridionale	5.87	ITIS043, ITCS055	A
26	1908	12	28	4	20	24	Calabria meridionale-Messina	7.1	ITIS013, ITCS016	A
27	1913	6	28	8	52	42	Calabria settentrionale	5.66	ITCS015	B
28	1928	3	7	10	55	16	Capo Vaticano	5.83	ITIS044, ITCS080	A
29	1947	5	11	6	32	17	Calabria centrale	5.7	ITES001	F
30	1998	9	9	11	28		Appennino Calabro-Lucano	5.64	ITDS070	D

Incorporating the static stress changes

The cumulative stress change ΔCFF is computed by adding the contributions from all the other sources that have ruptured after the latest known earthquake on a given segment. The computation is carried out all over the source area for each node of a dense rectangular grid (2x2 km). The methodology adopted is described in detail by Console et al. (2013). The algorithm for ΔCFF calculations assumes an Earth model with a half space characterized by uniform elastic properties. Considering the absence of direct information about the slip distribution for the causative earthquakes, in this study we have assumed for all of them a distribution consistent with a uniform stress drop (equal to 3.0 MPa) on the rectangle of the segment fault. We have calculated the slip distribution that satisfies the condition of zero slip on the edge and maximum at the center on the rectangle of the causative source (Console and Catalli, 2006).

The maximum value of the slip is defined through the relation $\Delta S_{max} = \frac{16}{\pi^2}\frac{M_0}{\mu W L}$

Where μ is the shear modulus of the elastic medium,
W and L the dimensions of the causative fault (width and length, respectively) and Mo is the seismic moment derived from the Kanamori and Anderson (1975) relation.
The effect of ΔCFF on the probability of future characteristic earthquakes assumes that the time elapsed since the previous earthquake is modified from t to t' by a shift, Δt, proportional to ΔCFF, that is

$$t' = t + \Delta t = t + \frac{\Delta CFF}{\dot{\tau}},$$

Where the tectonic stressing rate (τ) is assumed unchanged by the stress perturbation, estimated from the segment slip rate (V) and the area of the earthquake source (Console et al.,2008) as

$$\dot{\tau} = \frac{32\mu V}{\pi^2\sqrt{A}},$$

Where V is the long-term slip rate in meters per year, and A is rupture area.

List of the earthquakes of M>5.5 falling in the study area and associated to one or more of the different types of seismogenic sources. The Rank column is a way to establish how confident can be the association, and it is based on the overall knowledge of the earthquake. A description of the ranking method is given in Table ESM. Earthquakes are from the CPTI11 Catalogue (Rovida et al., 2011).

ABSOLUTE DIFFERENCE IN PGA BETWEEN TIME-DEP. & -INDEP. SEISMIC HAZARD

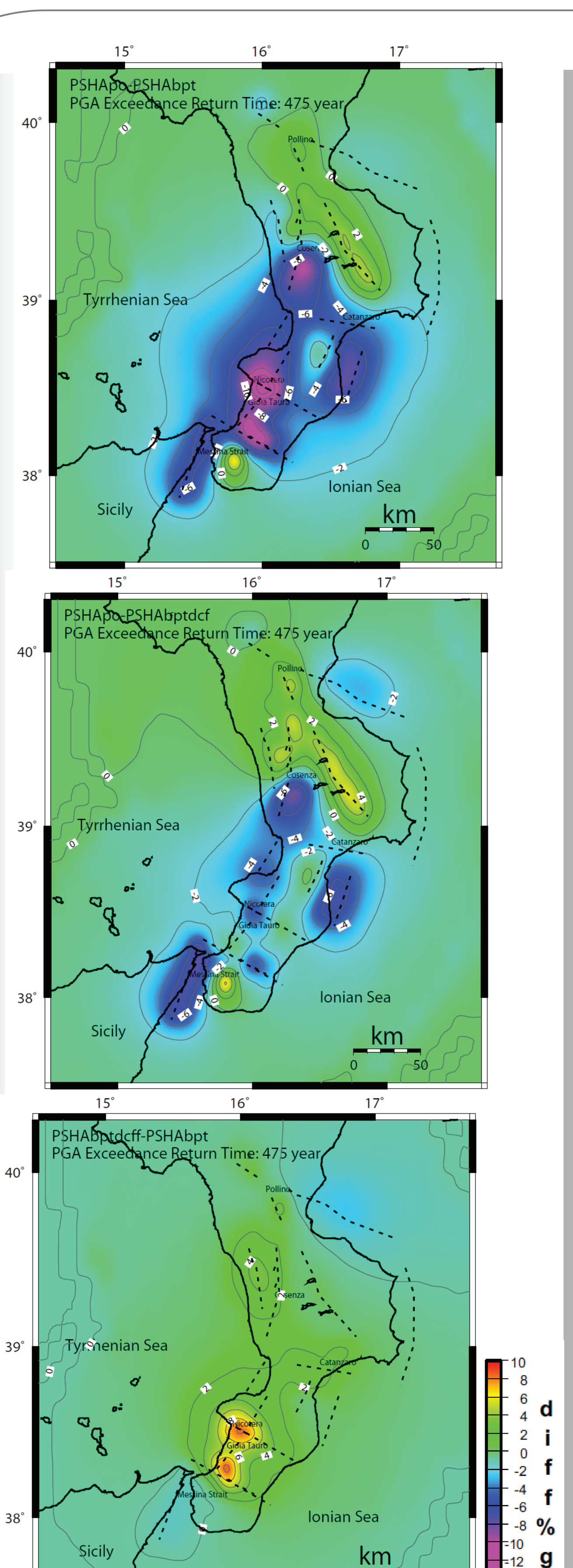

RELATIVE PERCENTAGE DIFFERENCE IN PGA BETWEEN TIME-DEP. & -INDEP. SEISMIC HAZARD

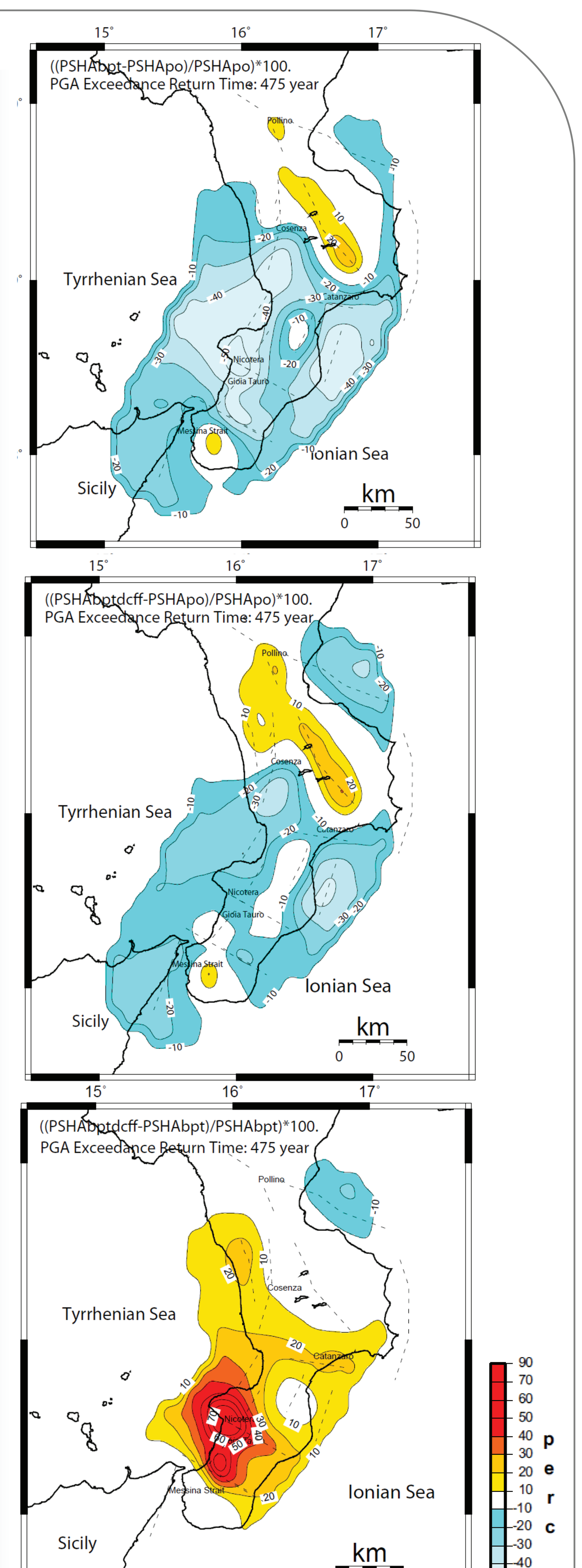

The absolute difference in PGA between the time-independent and –dependent fault based seismic hazard (probabilistic PGA having 10% probability of exceedance in the next 50 years starting from 2015); a) Absolute PGA variation between PSHApo-PSHAbpt; b) Absolute PGA variation between PSHApo-PSHAbptdcff; c) Absolute PGA variation between PSHAbptdcff-PSHAbpt.
The relative percentage difference (perc) in PGA (g%) between a) the Poisson and the BPT ; b) the Poisson and the BPT+ΔCFF; c) the BPT+ΔCFF and the BPT hazard models.

PEAK GROUND ACCELERATION MAPS IN 10% 50 YEARS

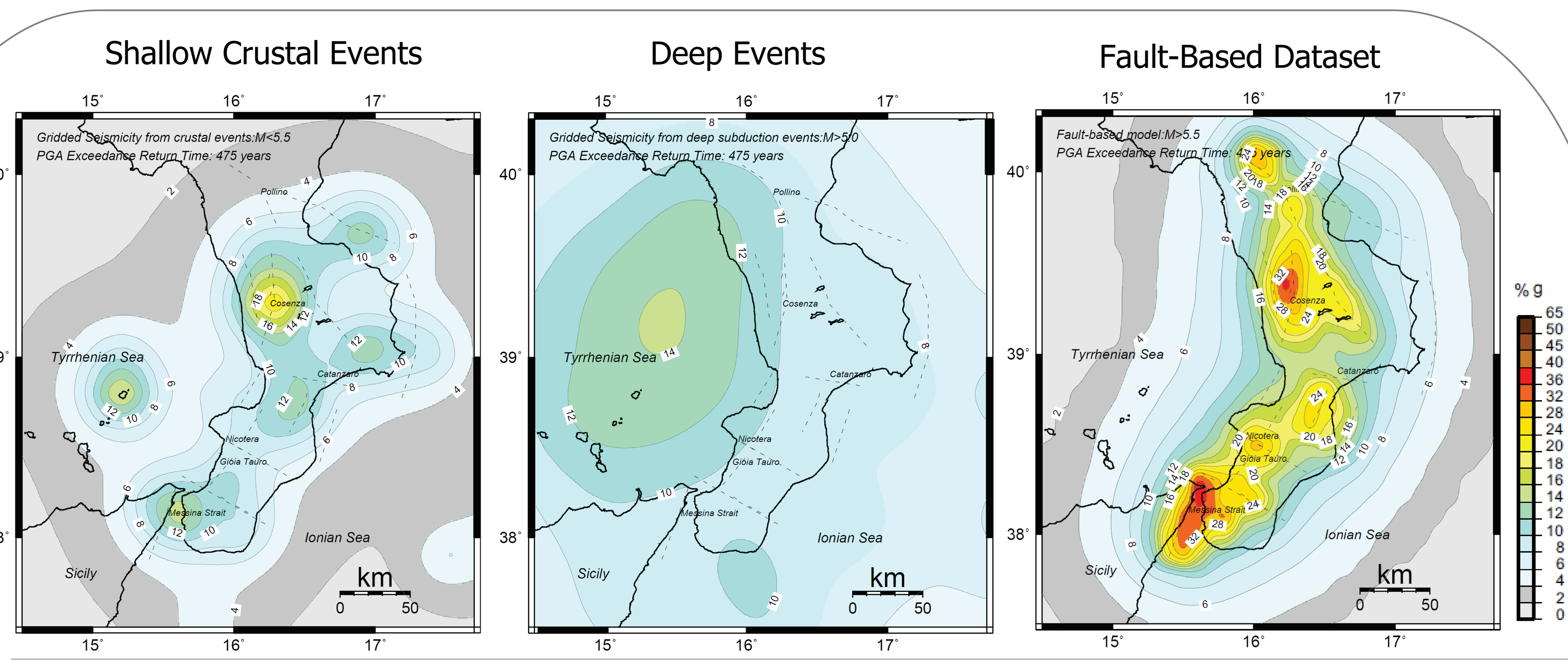

Maps of a) Time-independent (Poisson) probabilistic PGA (g%) having 10% probability of exceedance in 50 years, derived from the gridded seismicity from shallow crustal events; b) from deep events; c) from the fault-based information using the 50th percentiles occurrence probability of the characteristic earthquakes (M>5.5) in the Calabria region. For earthquakes with magnitude below Mw5.5 and Mw3.16, the source model is that of the fixed shallow and deep smoothed seismicity, respectively. For earthquakes with magnitude Mw5.5 or greater, the source model is that of the seismogenic sources with characteristic and floating faults. We followed the basic methodology and used the computer codes implemented by the U.S. Geological Survey (USGS) to construct the U.S. National Seismic Hazard Maps (Petersen at al. 2007)

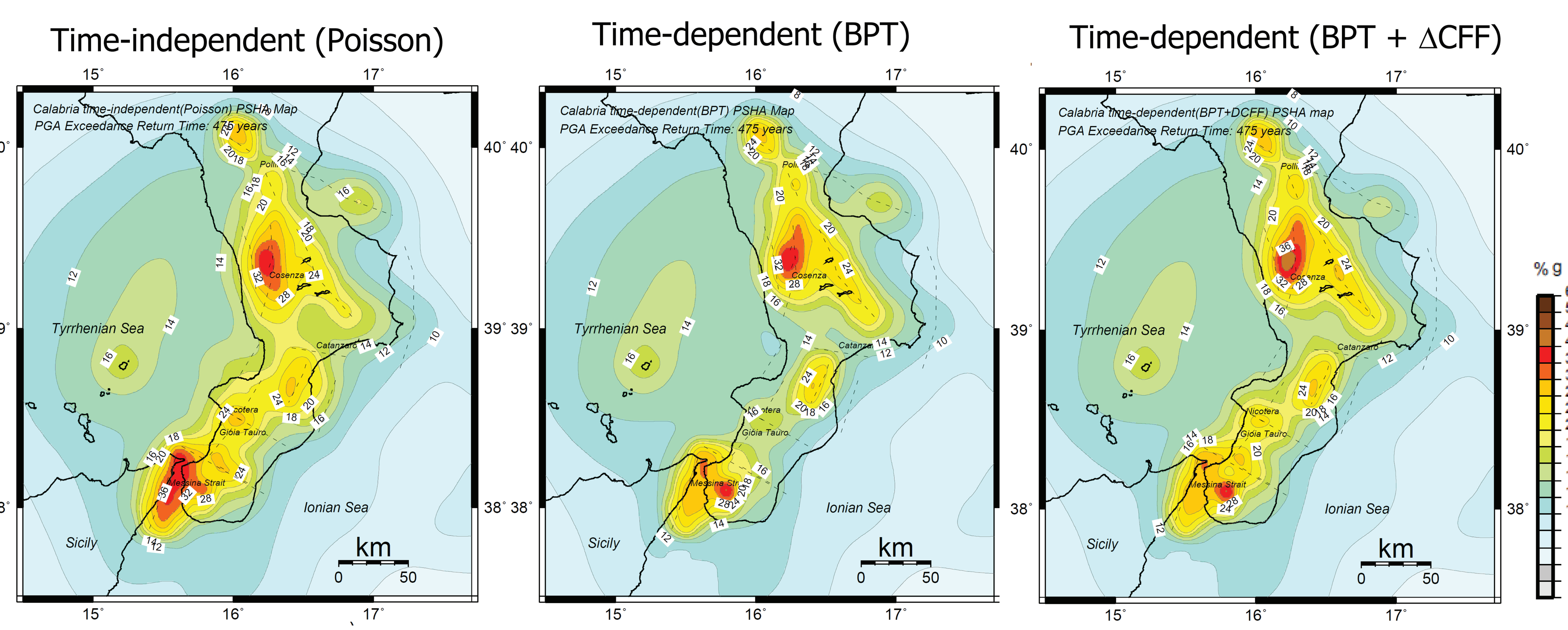

Resultant maps of PGA (g%) that has 10% chance being exceeded within 50 years in the Calabria region. Results are presented for three different earthquake occurrence probability models; a) Time-independent (Poisson); b) Time-dependent BPT; c) Time-dependent BPT+ΔCFF seismic hazard derived from both the gridded seismicity and the fault-based information using the 50th percentiles occurrence probability of the characteristic earthquakes (M>5.5) in the Calabria region. The four adapted Gmpes of the Next Generation Attenuation Models project, Boore and Atkinson (2008); the second derives from the Europe and Middle east GMPE model of Akkar and Bommer (2010); the third is the Italian GMPE model of Bindi et al. (2011); and the fourth is a global model, although mainly based on the Japanese data of Cauzzi and Faccioli (2008). In the case of the deep earthquakes we adopted only one GMPE derived by Lin and Lee (2008).

PROBABILITY OF OCCURRENCE IN THE NEXT 50 YRS

Source	Fault Type	Poisson	BPT 16th	BPT 50th	BPT 84th	BPT_ΔCFF_max 16th	BPT_ΔCFF_max 50th	BPT_ΔCFF_max 84th	ΔCFF_max Mpa	Slip rate mm/yr	M	Tr yr	Te yr	Te/Tr	strike	dip	rake
ITIS011	N	4.88E-02	1.12E-05	6.39E-03	3.10E-02	5.85E-03	3.88E-02	5.84E-02	1.04E+00	1.0	6.6	1000	232.00	0.23193	30.0	30.0	270.0
ITIS012	N	6.12E-02	2.33E-04	2.13E-02	5.74E-02	1.71E-02	6.32E-02	7.96E-02	7.35E-01	1.0	6.6	792	232.00	0.29285	30.0	30.0	270.0
ITIS013	N	6.54E-02	2.40E-08	8.81E-04	1.85E-02	2.42E-08	8.84E-04	1.85E-02	4.15E-04	2.0	7.0	739	107.00	0.14475	20.0	29.0	270.0
ITIS042	ON	9.52E-02	6.88E-05	2.05E-02	7.46E-02	3.23E-02	1.03E-01	1.25E-01	6.85E-01	0.5	5.8	500	121.00	0.24207	300.0	70.0	225.0
ITIS043	ON	7.09E-02	6.05E-08	1.26E-03	2.08E-02	6.31E-09	5.66E-04	1.47E-02	-6.31E-02	0.5	6.0	680	108.00	0.15882	300.0	70.0	225.0
ITIS044	OR	7.09E-02	3.60E-09	6.05E-04	1.43E-02	3.60E-09	6.05E-04	1.43E-02	-5.91E-05	0.5	6.0	680	87.00	0.12794	120.0	70.0	315.0
ITIS097	N	1.20E-01	1.50E-01	1.69E-01	1.75E-01	1.70E-01	2.01E-01	2.42E-01	8.07E-01	1.0	5.8	391	248.00	0.63348	180.0	65.0	270.0
ITIS098	N	1.32E-01	6.43E-02	1.58E-01	1.76E-01	9.06E-02	1.71E-01	1.79E-01	1.51E-01	1.0	5.9	353	180.00	0.50986	180.0	60.0	270.0
ITIS139	N	2.99E-02	5.11E-22	3.03E-08	1.45E-04	8.68E-22	3.61E-08	1.58E-04	7.67E-03	1.0	6.8	1647	110.00	0.06680	31.0	38.0	270.0
ITCS015A	N	1.71E-01	4.25E-02	1.55E-01	2.10E-01	4.25E-02	1.55E-01	2.10E-01	-2.47E-05	1.0	5.7	267	102.00	0.38187	180.0	60.0	270.0
ITCS015B	N	1.96E-01	2.13E-01	2.63E-01	2.70E-01	2.73E-01	3.12E-01	3.47E-01	4.93E-01	1.0	5.6	230	129.00	0.56187	180.0	60.0	270.0
ITCS016AB	N	3.53E-01	4.30E-01	5.92E-01	8.97E-01	4.29E-01	5.93E-01	9.00E-01	7.30E-01	2.0	5.6	115	235.00	2.04722	20.0	32.5	265.0
ITCS019A	R	2.07E-02	4.82E-23	1.55E-08	6.52E-05	2.38E-07	1.47E-03	1.05E-02	1.13E+00	0.5	6.6	2389	183.00	0.07661	185.0	30.0	90.0
ITCS033	N	3.53E-02	7.70E-04	1.76E-02	3.74E-02	1.96E-02	4.20E-02	4.77E-02	1.68E+00	0.6	6.2	1392	485.00	0.34854	160.0	60.0	270.0
ITCS033A	N	1.06E-01	1.46E-01	1.65E-01	1.81E-01	1.46E-01	1.65E-01	1.81E-01	2.43E-03	0.6	5.7	445	322.00	0.72329	160.0	60.0	270.0
ITCS053A	N	1.12E-01	7.39E-02	1.39E-01	1.51E-01	6.98E-02	1.37E-01	1.51E-01	-3.04E-02	1.0	6.0	419	224.00	0.53412	30.0	30.0	270.0
ITCS055	ON	7.09E-02	9.71E-02	1.07E-01	1.15E-01	1.01E-01	1.25E-01	1.74E-01	4.92E-01	0.5	6.0	680	485.00	0.71322	300.0	70.0	225.0
ITCS080	OR	7.09E-02	9.79E-02	1.09E-01	1.15E-01	1.03E-01	1.34E-01	2.02E-01	8.07E-01	0.5	6.0	680	485.00	0.71322	120.0	70.0	315.0
ITES002A	N	1.69E-01	2.32E-01	2.98E-01	4.59E-01	2.33E-01	2.93E-01	4.28E-01	-2.91E-01	1.0	5.7	270	272.00	1.00722	25.0	60.0	270.0
ITES002B	N	5.31E-02	2.39E-05	9.98E-03	4.18E-02	1.17E-05	8.11E-03	3.90E-02	-5.21E-02	1.0	6.7	916	232.00	0.25332	205.0	60.0	270.0
ITCS104	R	6.61E-02	8.27E-02	9.50E-02	9.80E-02	9.11E-02	1.41E-01	2.80E-01	4.74E+00	0.9	6.3	732	485.00	0.66289	290.0	45.0	77.5
ITCS104A	R	5.59E-02	5.35E-07	3.99E-03	2.99E-02	4.76E-03	4.46E-02	6.78E-02	1.67E+00	0.9	6.2	869	179.00	0.20608	290.0	45.0	77.5
ITCS111A	N	2.63E-02	7.84E-08	1.15E-03	1.04E-02	4.30E-06	3.70E-03	1.66E-02	3.61E-01	1.0	7.0	1876	377.00	0.20094	20.0	40.0	270.0
ITCS111B	N	9.79E-02	6.55E-04	3.42E-02	9.69E-02	7.30E-04	3.53E-02	9.78E-02	1.47E-02	1.0	6.1	485	145.00	0.29890	20.0	40.0	270.0
ITCS068	SS	1.36E-02	2.15E-07	1.37E-04	1.66E-03	1.82E-02	1.93E-02	1.97E-02	4.16E+00	0.5	6.9	3663	615.00	0.16791	100.0	80.0	350.0
ITDS030A	N	8.44E-02	3.54E-04	2.46E-02	7.51E-02	7.86E-02	1.14E-01	1.18E-01	1.52E+00	1.0	6.2	567	161.00	0.28395	342.5	50.0	270.0
ITDS053A	N	3.20E-02	2.42E-06	3.53E-03	2.10E-02	8.31E-06	5.03E-03	2.37E-02	1.23E-01	1.0	6.9	1539	377.00	0.24493	140.0	60.0	270.0
ITDS053B	N	4.83E-02	6.96E-02	8.35E-02	1.04E-01	6.95E-02	9.02E-02	1.38E-01	7.07E-01	1.0	6.7	1009	831.00	0.82342	166.0	60.0	270.0
ITDS053C	N	1.73E-01	2.38E-01	3.14E-01	4.93E-01	2.38E-01	3.15E-01	4.97E-01	4.86E-02	1.0	5.7	262	271.00	1.03254	133.0	60.0	270.0
ITDS065	N	1.50E-01	2.09E-01	2.43E-01	2.80E-01	2.09E-01	2.43E-01	2.79E-01	-2.11E-03	1.0	5.8	308	228.00	0.74002	197.5	50.0	260.0

Probabilities of occurrence for a 50-year period of time (2015–2065) for the seismogenic fault sources for both the Poisson and Time-dependent (BPT and BPT+ΔCFF) models. Uncertainties from a parameter are presented as a range between the 16th and 84th percentiles.

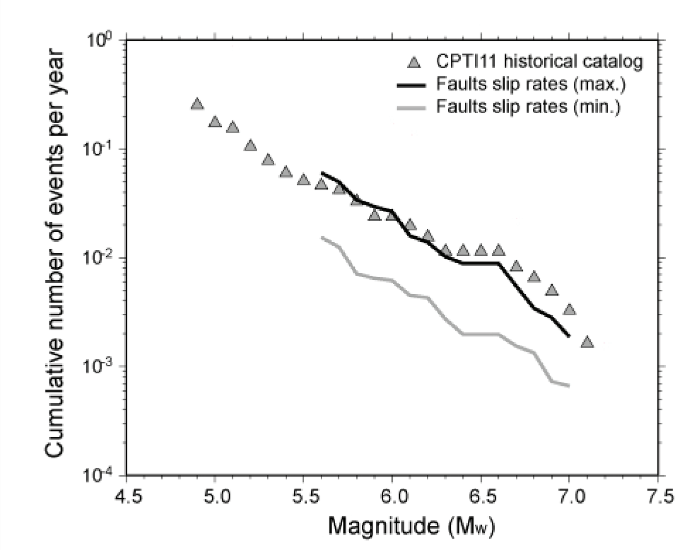

Cumulative number of events per year versus magnitude historically observed in Calabria (CPTI11) (triangles) and the predicted rates from characteristic faults– floating earthquakes (solid lines). The predicted numbers of events are calculated using minimum (gray line) and maximum slip (black line) rates on the all faults.

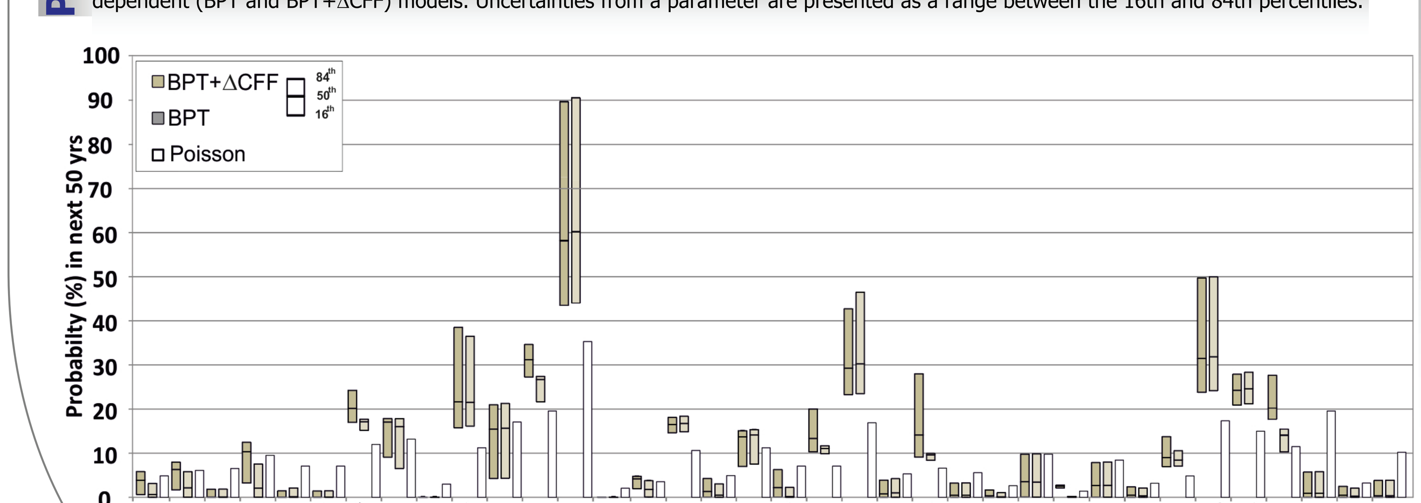

Occurrence probability on each Seismogenic Sources based on database developed in this study, over 50 years starting on January 1, 2015, according to Poisson, BPT and BPT + ΔCFF, considering the 16th, 50th and 84th percentile of Monte Carlo distribution. For each sources are also shown the Fault Kinematics (N for Normal, R for Reverse, ON for Oblique-Normal, OR for Oblique-Reverse and SS for Strike-Slip fault) and its mechanism,
Time Elapsed, the Mean Recurrence Time which is computed considering the maximum slip rate and the ratio between the Time Elapsed and Recurrence Time. We used maximum geologic slip rates in which minimizes the misfit between the characteristic model rate of earthquakes calculated from the geologic slip rate and the historic rate of earthquakes from the earthquake catalog.
The fault-based source model uses the dimensions and slip rates of mapped fault to develop magnitude–frequency estimates for characteristic earthquakes. In this study, the long-term slip rates are converted to the mean recurrence time in years (Tr) using the following equation; $T_r = \frac{M_0}{\mu V A}$

we modeled potential future earthquakes that could rupture the entire fault segment (full-source rupture) with a single event over the Individual Sources. The rate of floating rupture for each earthquake is calculated dividing the length of the fault by the total length of the rupture zone.

DISCUSSION AND CONCLUSION

Our results show that;
- The time-dependent maps differ by about 50% from the time-independent maps close to fault sources.
- From the traditional hazard maps we observed that the maximum PGA values associated with 10% probability of exceedance in 50 years vary between 0.32 g and 0.36 g in the Messina Straits and the Cosenza area while the time dependent analysis under the BPT model yields hazard results significantly lower (the absolute variation of PGA being about 0.1-0.15g) especially in the southern Calabria.

This difference becomes less pronounced considering the ΔCFF effect in the same area.
- However, we observed that a positive effect of ΔCFF is significant for several seismogenic sources in the southern Calabria.

The static stress change becomes critical when the faults close to the source under consideration produced the last event before its latest characteristic earthquake.
- Using the maximum values of ΔCFF, we observed that the PGA values increase around 0.1 g respect to those obtained using a simple renewal (BPT) model.

Although the percentage ratio between the seismic hazards computed using Poisson and renewal models is high (50%), the absolute PGA values are smaller in terms of the absolute difference in PGA being around 0.1-0.15 g along the southern Calabria seismogenic sources. The city of Cosenza and surrounding areas bear the highest seismic hazard with PGA around 0.4g in Calabria using both the time-dependent and time-independent models for the period of 2015-2065, this result is in agreement with previous study findings by Peruzza et al. (1997).

REFERENCES

Akkar S, Bommer JJ (2010) Empirical equations for the prediction of PGA, PGV, and spectral accelerations in Europe, the Mediterranean, and the Middle East. Seismol Res Lett 81(2):195-206. doi: 10.1785/gssrl.81.2.195

Akinci A, Galadini F, Pantosti D, Petersen M, Malagnini L, Perkins D (2009) Effect of Time Dependence on Probabilistic Seismic-Hazard Maps and Deaggregation for the Central Apennines, Italy. B Seismol Soc Am 99(2A):585-610. doi: 10.1785/0120080053

Akinci, A, Perkins, D, Lombardi AM, and Basili R (2010) Uncertainties in the estimation of the probability of occurrence of strong earthquakes from individual seismological sources in the Apennines, Italy, J. Seismol.,14, 95-117

Akinci A (2010) HAZGRIDX: earthquake forecasting model for ML ≥ 5.0 earthquakes in Italy based on spatially smoothed seismicity. Ann Geophys-Italy 53(3):51-61. doi: 10.4401/ag-4811

Bindi D, Pacor F, Luzi L, Puglia R, Massa M, Ameri G, Paolucci R (2011) Ground motion prediction equations derived from the Italian strong motion database. B Earthq Eng. doi: 10.1007/s10518-011-9313-z

Boore DM, Atkinson GA (2008) Ground Motion prediction equations for the average horizontal component of PGA, PGV, PGD, and 5\% damped PSA art spectral periods between 0.01 s and 10.0 s. Earthq Spectra 24(1):99-138

Console, R, Catalli, F (2006) A rate-state model for aftershocks triggered by dislocation on a rectangular fault: a review and new insights, Annals of Geophysics 49(6): 1259-1263

Console R, Murru M, Falcone G, Catalli F (2008) Stress interaction effect on the occurrence probability of characteristic earthquakes in Central Apennines. J Geophys Res 113(B08313). doi: 10.1029/2007JB005418

Console R, Murru M, Falcone G (2010) Perturbation of earthquake probability for interacting faults by static Coulomb stress changes. J Seismol 14:67-77. doi: 10.1007/s10950-008-9149-4

Console R, Falcone G, Murru M, Karakostas V, Papadimitriou E, Rhoades D (2013) Renewal Models and co-seismic stress transfer in the Corinth Gulf, Greece, Fault System. J Geophys Res 118:1-119. doi: 10.1002/jgrb.50277

Rovida A, Camassi R, Gasperini P, Stucchi M (eds) (2011) CPTI11, the 2011 version of the Parametric Catalogue of Italian Earthquakes, Milano, Bologna. http://emidius.mi.ingv.it/CPTI. doi:10.6092/INGV.IT-CPTI11. Accessed 1 July 2014

Petersen MD, Cao T, Campbell KW, Frankel AD (2007) Time-independent and Time-dependent Seismic Hazard Assessment for the State of California: Uniform California Earthquake Rupture Forecast Model 1.0 Seismological Research Letters 78:99-109Peruzza L, Pantosti D, Slejko D, Valensise G (1997) Testing a new hybrid approach to seismic hazard assessment: an application to the Calabria Arc (Southern Italy). Natural Hazard 14:113-126

Lin PS, Lee CT (2008) Ground-motion attenuation relationships for subduction zone earthquakes in northeastern Taiwan. Bull Seismol Soc Am 98:220-240

Cauzzi C, Faccioli E (2008) Broadband (0.05 to 20s) prediction of displacement response spectra based on worldwide digital records. J Seismol 12:453-475